The negative piezoelectric effect of the ferroelectric polymer poly(vinylidene fluoride)

Katsouras, Ilias; Asadi, Kamal; Li, Mengyuan; van Driel, Tim B.; Kjaer, Kasper S.; Zhao, Dong; Lenz, Thomas; Gu, Yun; Blom, Paulw. M.; Damjanovic, Dragan

Published in:
Nature Materials

DOI:
10.1038/NMAT4423

ARTICLES
PUBLISHED ONLINE: 5 OCTOBER 2015 | DOI: 10.1038/NMAT4423
nature materials

The negative piezoelectric effect of the ferroelectric polymer poly(vinylidene fluoride)

Ilias Katsouras[1,2], Kamal Asadi[1], Mengyuan Li[3,4], Tim B. van Driel[5], Kasper S. Kjær[5], Dong Zhao[1], Thomas Lenz[1], Yun Gu[5], Paul W. M. Blom[1], Dragan Damjanovic[6], Martin M. Nielsen[5] and Dago M. de Leeuw[1,7]*

Piezoelectricity describes interconversion between electrical charge and mechanical strain. As expected for lattice ions displaced in an electric field, the proportionality constant is positive for all piezoelectric materials. The exceptions are poly(vinylidene fluoride) (PVDF) and its copolymers with trifluoroethylene (P(VDF-TrFE)), which exhibit a negative longitudinal piezoelectric coefficient. Reported explanations exclusively consider contraction with applied electric field of either the crystalline or the amorphous part of these semi-crystalline polymers. To distinguish between these conflicting interpretations, we have performed *in situ* dynamic X-ray diffraction measurements on P(VDF-TrFE) capacitors. We find that the piezoelectric effect is dominated by the change in lattice constant but, surprisingly, it cannot be accounted for by the polarization-biased electrostrictive contribution of the crystalline part alone. Our quantitative analysis shows that an additional contribution is operative, which we argue is due to an electromechanical coupling between the intermixed crystalline lamellae and amorphous regions. Our findings tie the counterintuitive negative piezoelectric response of PVDF and its copolymers to the dynamics of their composite microstructure.

Piezoelectricity describes the conversion of electrical charge to mechanical strain and vice versa. The direct piezoelectric effect is observed as a change in surface charge density of a material in response to an external mechanical stress. The effect is reversible; the thermodynamic equivalent is a change in dimension on applying an electric field.

A large piezoelectric coefficient, describing the change in spontaneous electrical polarization with applied mechanical stress, is obtained for ferroelectric materials. When an electric field is applied in the direction of the polarization most ferroelectric materials will expand. However, there is one well-known exception. The ferroelectric polymer poly(vinylidene fluoride) (PVDF) and its copolymers with trifluoroethylene P(VDF-TrFE) show an unusual negative longitudinal piezoelectric effect. Counterintuitively, these polymers contract in the direction of an applied electric field. The two opposite behaviours are schematically represented in Fig. 1.

It has been shown that the strain in PVDF varies as the square of the polarization[1]. Hence the origin of piezoelectricity is electrostriction biased by the spontaneous polarization. A negative piezoelectric coefficient was extracted. At present, two contradicting microscopic models have been proposed; the piezoelectric response is attributed to either the crystalline or the amorphous part of the semi-crystalline polymer.

Quantum chemical calculations for the ferroelectric β-phase of PVDF have shown that for a single crystal the piezoelectric effect is negative[2]. When an electric field is applied perpendicularly to the PVDF chain, the backbone stretches and its height is compressed. The lattice constant is reduced. The calculated coefficient agrees with the value experimentally determined on bulk samples, implying that the change in lattice constant fully accounts for the change in film thickness. This is surprising as PVDF is a semi-crystalline polymer (∼50%). Apparently in this analysis the amorphous part was disregarded.

On the other hand, the commonly used explanation for the negative piezoelectric effect of PVDF, the so-called dimensional model, assumes that the dipoles are rigid and retain their fixed moment and orientation during mechanical deformation[3–5]. A detailed description is given in Supplementary Section 2. This model basically describes the displacement of surface electrodes in the field of fixed PVDF dipole moments. Piezoelectricity is then due to a change in volume of the amorphous part of the sample. In the dimensional model the crystalline part is disregarded. In summary, according to the current interpretations, the piezoelectric response of PVDF comes either from the crystalline part or from the amorphous part; curiously, each seems to fully account for the experimentally observed piezoelectric response.

The piezoelectric properties of P(VDF-TrFE) have until now been determined macroscopically on films, by measuring the change in film thickness on application of an electric field. To reveal the microscopic origin of the negative piezoelectric effect, it is not the macroscopic change in film thickness but the change in lattice constant that has to be measured as a function of electric field. However, this requires addressing selectively the contribution of the crystalline part. To that end, we performed *in situ* dynamic X-ray diffraction measurements.

There are severe experimental challenges in performing these X-ray measurements: the minute changes can be determined only dynamically, by measuring the diffracted X-ray intensity *in situ*, as

[1]Max-Planck Institute for Polymer Research, Ackermannweg 10, 55128 Mainz, Germany. [2]Holst Centre, High Tech Campus 31, 5656 AE, Eindhoven, The Netherlands. [3]Zernike Institute for Advanced Materials, University of Groningen, Nijenborgh 4, 9747 AG, Groningen, The Netherlands. [4]Electronic Information Industry, CCID Thinktank, China Center for Information Industry Development No. 27, Wanshou Road, 100846 Beijing, China. [5]Department of Physics, Technical University of Denmark, DK-2800 Lyngby, Denmark. [6]Ceramics Laboratory, Swiss Federal Institute of Technology—EPFL, 1015 Lausanne, Switzerland. [7]King Abdulaziz University, Abdullah Sulayman, 22254 Jeddah, Saudi Arabia. *e-mail: deleeuw@mpip-mainz.mpg.de

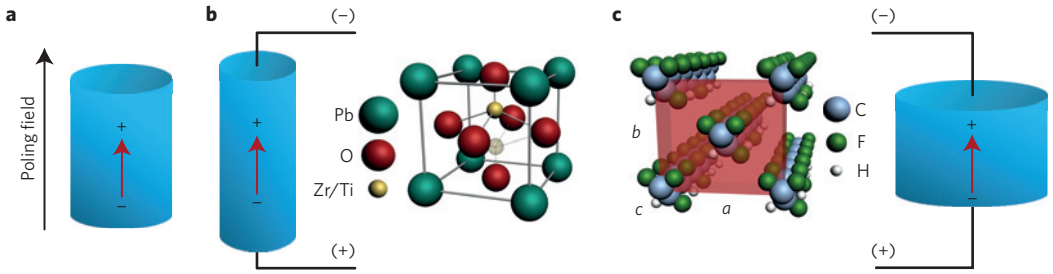

Figure 1 | Piezoelectricity. Schematic illustration of strain on application of an electric field in a poled ferroelectric material. **a**, The initial state. **b**, When an electric field is applied in the direction of the polarization in a material with a positive piezoelectric coefficient, such as lead zirconate titanate (PZT), the material expands. **c**, The counterintuitive behaviour of PVDF and its copolymers. These materials contract, exhibiting a negative piezoelectric coefficient. Schematic crystal structures are shown in **b** and **c**.

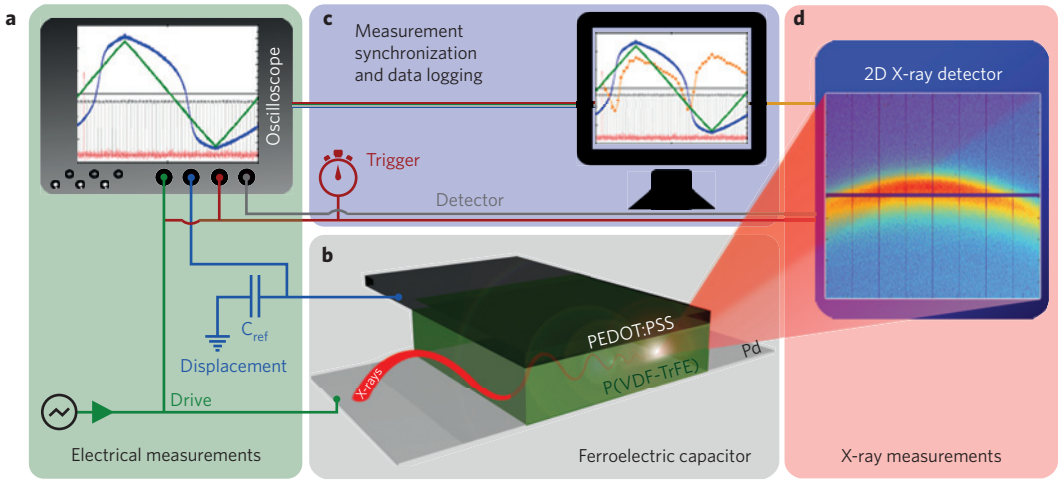

Figure 2 | Dynamic *in situ* XRD measurement. a,**b**, An a.c. voltage is applied over a P(VDF-TrFE) capacitor. The drive signal and the electric displacement of the ferroelectric capacitor are measured as a function of time and recorded using a Sawyer–Tower set-up. **c**,**d**, On application of the a.c. signal on the capacitor, a trigger signal is sent to the X-ray detector, starting an exposure-series of 10,000 images. The 2D X-ray diffraction pattern is measured under grazing incidence synchrotron X-ray irradiation, to enhance the signal-to-noise ratio. The trigger and detector timing data are recorded by the oscilloscope and all data are transferred to a computer.

a function of a time-varying electric field. Only then can the strain, defined as the relative change in lattice constant, be obtained by statistical averaging over thousands of acquired X-ray diffractograms. Furthermore, the strain is related to the ferroelectric polarization. Hence, to arrive at a quantitative description of the piezoelectric effect in P(VDF-TrFE), the changes in lattice constant have to be measured simultaneously with the ferroelectric polarization, yielding constraints on data acquisition and synchronization. Finally, the diffracted X-ray intensity depends on the atomic structure factors, which for the constituent atoms of P(VDF-TrFE) are small. High-intensity X-rays from a synchrotron are a prerequisite to obtain a decent signal-to-noise ratio.

Here we report dynamic *in situ* X-ray diffraction measurements on P(VDF-TrFE) capacitors while an electric field is applied. We simultaneously extract the lattice strain and polarization as a function of electric field. The strain is dominated by electrostriction, but an additional contribution has to be included to quantitatively describe the strain for all values of the electric field. This additional contribution can be due to any process that yields a strain that depends linearly on electric field. We argue, based on the microstructure, that the origin is an electromechanical coupling between the intermixed crystalline lamellae and amorphous regions of the semi-crystalline polymer. Changes in lattice constant on application of an electric field are coupled to volume changes in the amorphous regions and vice versa. We show that the model developed, unambiguously and quantitatively describes reported strain measurements and we discuss why the piezoelectric coefficient is negative.

The experiment is schematically described in Fig. 2. Details are presented in the Supplementary Information. Grazing incidence X-ray diffraction (GI-XRD) measurements were performed on P(VDF-TrFE) capacitors. The design of the capacitors was optimized to avoid parasitic diffraction patterns that interfere with the diffraction of P(VDF-TrFE) (Supplementary Section 4). An a.c. voltage was applied over the capacitor and the electric displacement current was measured as a function of time. Crucial for the present experiment is that the X-ray diffractogram is measured as a function of time as well, for which we used a time-resolved 2D X-ray detector[6,7].

On application of an a.c. voltage on the capacitor, a trigger signal was sent to the X-ray detector starting an exposure-series of 10,000 images. The specular scattering images recorded were azimuthally integrated and exposures pertaining to the same time-bin relative to the driving frequency were averaged. An example of the signal after integration and binning is presented in Fig. 3a. A clear modulation of the Bragg peak is observed. The wavevector at about 1.3 $Å^{-1}$, shown in Fig. 3b, is characteristic of the combined (110)/(200) diffraction of the monoclinic low-temperature phase of P(VDF-TrFE) (Supplementary Section 4). Both the (110) and (200) reflections are perpendicular to the polymer chain direction and thus sensitive to structural dynamics in the transverse-chain direction of the crystals. The electrical data collected from the oscilloscope are shown in Fig. 3c. The driving field (green) and

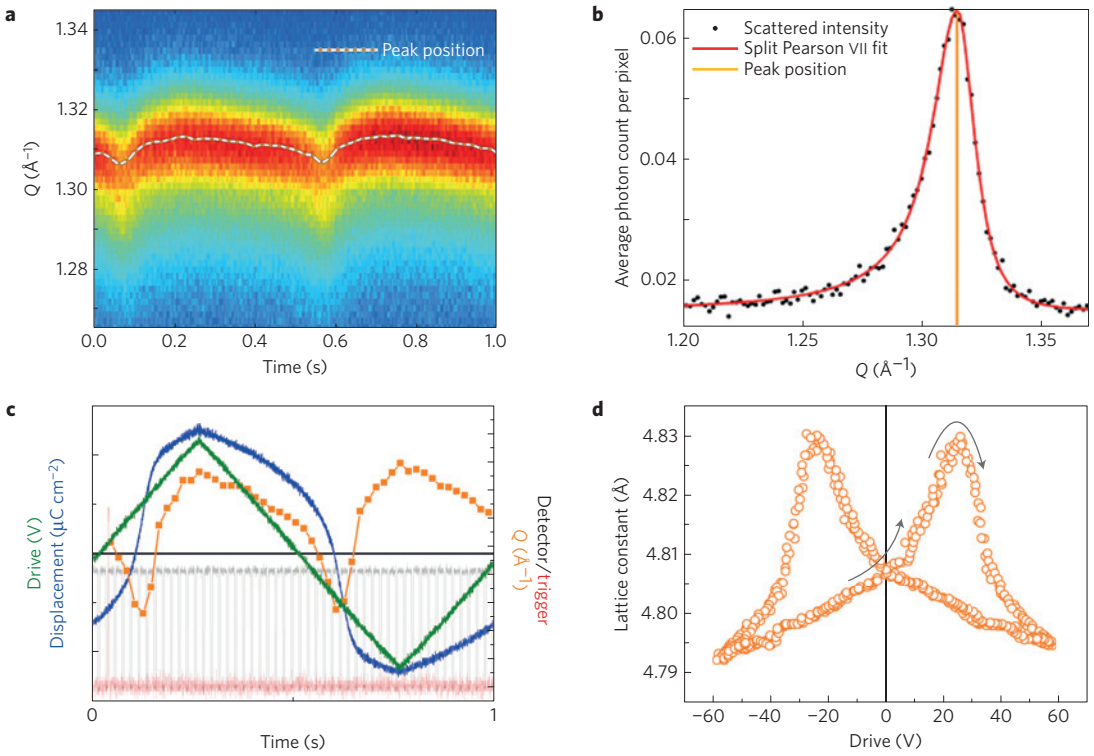

Figure 3 | Data acquisition. a, An example of a processed X-ray signal, showing the scattering vector, *Q*, as a function of time. Specular scattering images recorded were azimuthally integrated and exposures pertaining to the same time-bin were averaged. The capacitor was driven with a 1 Hz triangular waveform. A clear oscillation of the Bragg peak position is observed. **b**, The extracted (110)/(200) diffraction peak of the monoclinic low-temperature phase of P(VDF-TrFE). The red line is a single Split Pearson VII fit to the Bragg peak. **c**, Recorded data from the oscilloscope, showing the 1 Hz drive signal (green) and the displacement current of the ferroelectric capacitor (blue). The trigger signal (red) starts the series of 10,000 X-ray exposures at, for example, 100 Hz, mirrored by the grey lines. The synchronized diffraction data are presented in orange. **d**, Lattice constant, derived from the scattering vector *Q*, as a function of applied a.c. voltage, following from the synchronized data of **c**. Arrows indicate the sweep direction.

polarization (blue) yield the ferroelectric hysteresis loop. The trigger pulse (red) and the TTL signal from the detector that mirrors the exposures (grey), allow synchronization of the X-ray data (dots) with the electrical measurements. The out-of-plane lattice constant, the *b*-axis, which is directed along the sample surface normal and the electric field, is presented as a function of applied a.c. voltage in Fig. 3d. The modulation of the lattice constant is about 0.5%.

The electric displacement as a function of electric field is presented in Fig. 4a. The strain calculated as the relative change in lattice constant, $\Delta l/l_0$, where l_0 is the value at zero electric field, is presented in Fig. 4b. The strain, normalized to zero at zero electric field, depends on the relative orientation of electric field and polarization. For clarity the corresponding parts in the displacement versus field (*D*–*E*) and strain versus field (*S*–*E*) loops are presented with identical colours. Looking at Fig. 4b, we start at zero bias with a negatively poled film and increase the electric field (yellow data points). The film expands. The expansion continues until the coercive field, where the polarization switches direction (transition from yellow to red data points). Then the polarization and electric field are aligned in the same direction and the film rapidly contracts (red data points). As a final result, the strain as a function of electric field shows a typical butterfly shape. The strain measurement shows the negative longitudinal piezoelectric effect; the unit cell contracts when an electric field is applied in the direction of the polarization.

To understand the origin of the negative piezoelectric effect the strain measurements have to be quantitatively interpreted. The change in lattice constant can be due to elastic strain, Maxwell strain and/or piezoelectric strain. The elastic strain describes the deformation of a sample under applied mechanical stress. This direct stress–strain contribution can be disregarded, as external mechanical stress is not applied. Internal mechanical stress, however, can be relevant in the sample through electromechanical coupling, as will be discussed later. The compressive Maxwell strain is due to the electrostatic Coulomb attractive force between oppositely charged faces of a dielectric. However, in ferroelectric capacitors the surface charge density is compensated by countercharges of either polarity in the corresponding adjacent electrode[8]. Hence the Maxwell strain can be disregarded as well. In Supplementary Section 8 we show that clamping can be ignored.

The piezoelectric strain in a ferroelectric single crystal with centrosymmetric paraelectric phase is typically obtained from a free energy expansion in a Taylor series[9] with respect to either electric displacement, *D*, or polarization, *P*. Here we take *D* as the fundamental variable[10]. Odd terms in the expansion vanish by symmetry[11]. The electric displacement is the sum of the induced, P_i, and spontaneous, P_s, polarization, both of which are functions of electric field:

$$D = P_i + P_s = \varepsilon_r \varepsilon_0 E\acute{p} + P_s$$

where ε_r and ε_0 are the relative and vacuum permittivity. $\acute{p}$ is a parity function, with values of -1 or $+1$, to account for the relative orientation of electric field and spontaneous polarization, which are independent for a poled piezoelectric material (Supplementary Section 9.2). The first non-vanishing term of the Taylor series expansion of the strain, S_{33}, also abbreviated as *S*, then reads:

$$S_{33} = Q_{33}D^2 = Q_{33}(\varepsilon_r \varepsilon_0 E\acute{p} + P_s)^2$$
$$= 2Q_{33}\varepsilon_r \varepsilon_0 P_s E\acute{p} + Q_{33}P_s^2 + Q_{33}\varepsilon_r^2 \varepsilon_0^2 E^2 \quad (1)$$

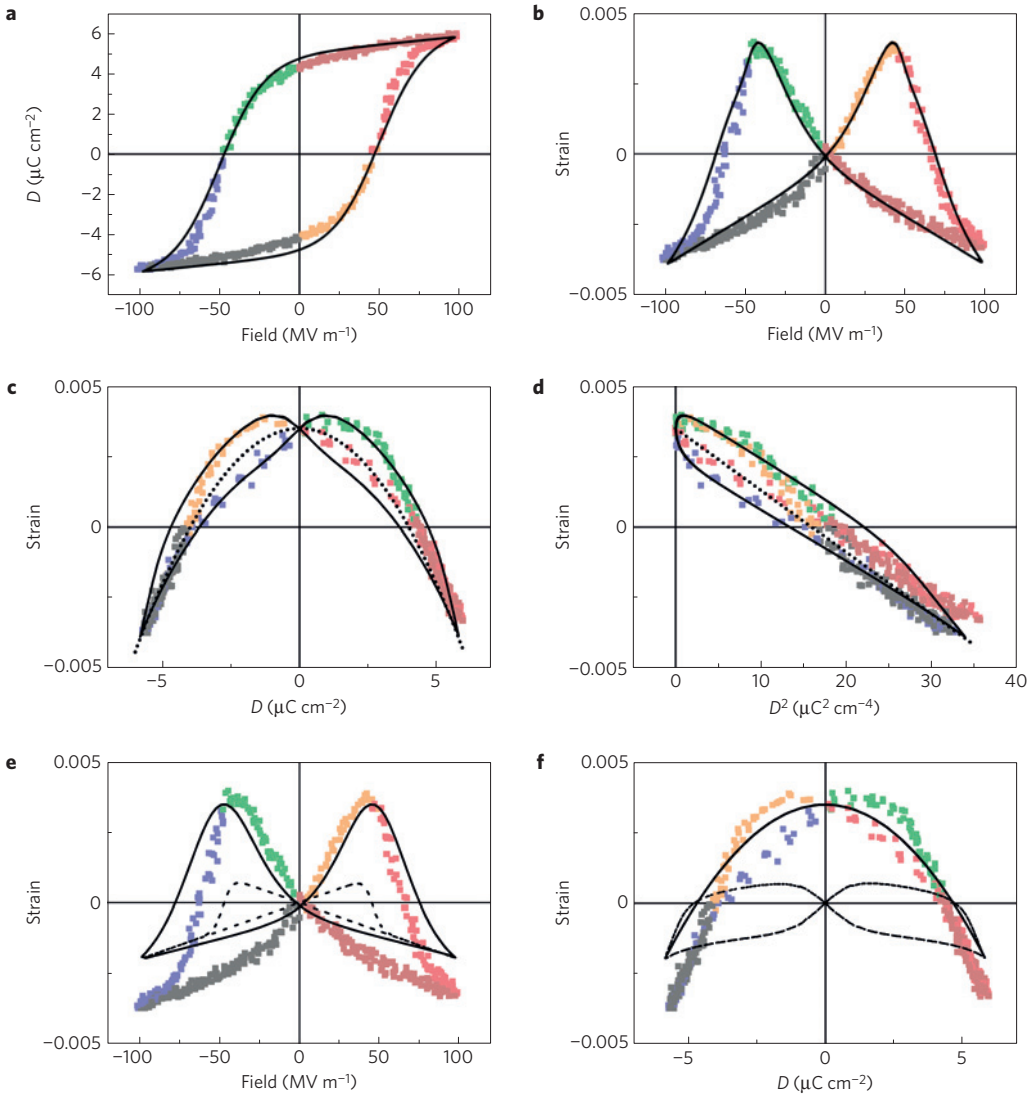

Figure 4 | Strain and displacement characteristics of P(VDF-TrFE). a, Ferroelectric displacement as a function of applied electric field (D–E). The solid curve is a fit according to the empirical model presented in Supplementary Section 8.1. Here the capacitor was driven with a 1 Hz triangular waveform. **b**–**d**, Strain as a function of field (S–E) (**b**), displacement (S–D) (**c**), and displacement squared (S–D^2) (**d**). The data have been colour-coded to facilitate the correspondence between the different representations. The dotted lines are the fits according to equation (1). The black solid lines are a fit according to equation (2). The fit constants are presented in Table 1. **e**,**f**, The experimental strain and the contributions of the electrostrictive term, $Q_{33}D^2$ (solid lines), and the coupling term, $d_{coupling}E\acute{p}$ (dotted lines), as a function of electric field (**e**) and electric displacement (**f**). The strain is clearly dominated by electrostriction. The additional term, $d_{coupling}E\acute{p}$, becomes increasingly important with increasing electric field, and introduces the experimentally observed hysteresis.

Table 1 | Extracted piezoelectric coefficients.

Material	E_c (MV m^{-1})	P_r (μC cm^{-2})	Q_{33} (m^4 C^{-2})	$d_{coupling}$ (pm V^{-1})	$2Q_{33}\varepsilon_0\varepsilon_r P_r$ (pm V^{-1})	d_{33} (pm V^{-1})
P(VDF-TrFE)	55	4.3	−1.5	−20	−11.4	−31.4
β-PVDF	58	5.5	−1.3	−25	−12.7	−37.7

Values in the top row are extracted from modelling the present dynamic *in situ* X-ray measurements on P(VDF-TrFE), as shown in Fig. 4. Values in the bottom row are extracted from modelling reported strain measurements on bulk films of β-PVDF (ref. 1). The relative error of the fit parameters, as calculated from an unweighted linear regression analysis, is less than 0.5% for E_c and P_r, less than 4% for $d_{coupling}$, and less than 2% for Q_{33}. The relative error of the total d_{33}, calculated by the propagation of uncertainty, is less than 3%.

where we have made use of the fact that $\acute{p}^2$ equals unity. Q_{33} is the coefficient of electrostriction, a universal property of solid and liquid dielectrics[12,13]. It is a fourth-rank tensor, commonly written with two indices following Voigt's notation. The first term on the right hand side of equation (1) corresponds to the piezoelectric effect, with the piezoelectric coefficient equal to $2Q_{33}\varepsilon_r\varepsilon_0 P_s$. The piezoelectric effect can thus be understood as the electrostriction biased by the spontaneous polarization. The second term $Q_{33}P_s^2$ describes the spontaneous strain. The last term, $Q_{33}\varepsilon_r^2\varepsilon_0^2E^2$, is referred to as the pure electrostrictive contribution. For ferroelectric materials this term is small and typically disregarded. We note that equation (1) has been widely used to fit the strain as measured

interferometrically on uniaxially drawn PVDF films[1]. However, only data far from the coercive field could be described. The hysteresis and the strain value at zero displacement could not be accounted for. Below we show that for the analysis of our lattice strain measurements an additional contribution to the strain has to be included. In Supplementary Section 11 we show that the full reported data set, including the hysteresis, can then unambiguously and quantitatively be described.

From the independent measurements of Fig. 4a,b, we can directly plot the strain as a function of electric displacement, by elimination of the electric field. We note that, although both strain and electric displacement have hysteresis when presented as a function of electric field, the strain as a function of displacement is a hysteresis-free parabola, as predicted by equation (1) for a single crystal and as indicated by the dotted line in Fig. 4c. Similarly, the strain as a function of the displacement squared should be a straight line, as indicated in Fig. 4d. The experimental data of Fig. 4c,d however, do show hysteresis.

The strain is derived from the change in lattice constant of the P(VDF-TrFE) crystals. Surprisingly, however, the strain in P(VDF-TrFE) cannot be described by the single-crystal formalism, equation (1) (ref. 11). The hysteresis in lattice strain implies that there must be an additional contribution to the piezoelectric effect. To model the strain, we therefore include an extra term, $d_{\text{coupling}}E\acute{p}$, where d_{coupling} is a phenomenological fit constant and E is the applied electric field. $\acute{p}$ is again the parity function, which takes into account that the sign of the strain depends on the relative orientation of electric field and polarization. Such an extra term, which adds to the lattice strain, can be found in the description of the piezoelectric response in inorganic polycrystalline materials. In piezoelectric ceramics it has been shown that the strain originating from piezoelectrically induced mechanical interactions among crystallites superimposes linearly on the lattice strain[14]. We adopt this additive approach, noting that in PVDF and its copolymers the crystallites are intertwined with the soft, non-piezoelectric matrix; intergranular strain is not immediately expected. The microscopic origin of this additional contribution to the strain will be discussed in detail below. Using this approach, the hysteresis can be quantitatively explained. The lattice strain now reads:

$$S_{33} = d_{\text{coupling}}E\acute{p} + Q_{33}D^2 = (d_{\text{coupling}} + 2Q_{33}\varepsilon_r\varepsilon_0 P_s)E\acute{p} + Q_{33}P_s^2 + Q_{33}\varepsilon_r^2\varepsilon_0^2E^2 \quad (2)$$

and the linear piezoelectric coefficient, d_{33}, extracted at low electric fields, where the spontaneous polarization can be considered constant and equal to the remanent polarization, is given by:

$$d_{33} = \left.\frac{\mathrm{d}S_{33}}{\mathrm{d}(\acute{p}E)}\right|_{E=0} = d_{\text{coupling}} + 2Q_{33}\varepsilon_r\varepsilon_0 P_r$$

Extraction of piezoelectric- and electrostrictive coefficients from the strain data of Fig. 4 starts with a quantitative description of polarization as a function of electric field. To that end we use an empirical model[15,16] that has been previously used to quantitatively describe ferroelectric capacitors[17]. The details are presented in Supplementary Section 9.1. There are only three empirical parameters—namely, remanent polarization, saturation polarization and coercive field. The solid curve in Fig. 4a is a fit to the experimental displacement versus field data. Once the D–E relation is known, we can simultaneously fit the strain versus field (S–E) and strain versus displacement (S–D, S–D^2) characteristics (equation (2)). The fits are presented by the solid lines in Fig. 4b–d. A good agreement is obtained. The fit constants are presented in Table 1. The extracted coupling contribution to the piezoelectric coefficient, d_{coupling}, is $-20\,\text{pm V}^{-1}$ and the extracted piezoelectric contribution, $2\varepsilon_0\varepsilon_r Q_{33}P_s$, is $-11\,\text{pm V}^{-1}$. The extracted total value of d_{33} is then $-31\,\text{pm V}^{-1}$. We have extracted the same value from dynamic *in situ* XRD measurements at low electric field (Supplementary Section 10.3). We performed the same analysis on reported strain measurements of ferroelectric β-PVDF films (Supplementary Section 11; ref. 1). We show that the strain can quantitatively be interpreted, for all values of the applied electric field, including hysteresis. The extracted parameters, presented in Table 1, are comparable to those of the copolymer.

Table 1 shows that the total value extracted for d_{33}, of about $-30\,\text{pm V}^{-1}$, is comparable to values derived from strain measurements of bulk samples using, for example, interferometry[1,18]. This implies that macroscopic piezoelectricity is dominated by the change in lattice constant. This conclusion is surprising. Piezoelectricity in polycrystalline inorganic ferroelectrics is dominated by extrinsic contributions such as domain wall motion[19,20]. The present analysis shows that for P(VDF-TrFE) the contribution from the change in lattice constant is dominant.

To illustrate that the strain is dominated by electrostriction we present in Fig. 4e,f the experimental strain and the contributions of the electrostrictive and coupling terms, as functions of the electric field and electric displacement, respectively. The experimental strain is replotted from Fig. 4b,c. The electrostrictive contribution, presented as the solid lines, is taken as $Q_{33}D^2$. The dotted lines indicate the contribution of the coupling term, $d_{\text{coupling}}E\acute{p}$. The strain is clearly dominated by electrostriction. The additional term, $d_{\text{coupling}}E\acute{p}$, becomes increasingly important with increasing electric field and introduces the experimentally observed hysteresis.

The electrostrictive coefficient, Q_{33}, is expected to be negative owing to the different force constants for the intra- and inter-chain interactions[21]. Application of a positive stress perpendicular to the chains mainly increases the distance between the chains, owing to the relatively weak van der Waals and electrostatic interactions between the chains, as compared to the strong covalent bonds within the chains. The thickness increase thus results in a decrease of the dipole density, which causes a concomitant decrease of the compensating charges on the electrodes. Consequently the electrostrictive coefficient, Q_{33}, is negative. The piezoelectric coefficient then is also negative, as for a single crystal, d_{33}, is equal to $2\varepsilon_r\varepsilon_o Q_{33}P_r$. This dipole-induced piezoelectricity[21] mechanism is confirmed by quantum mechanical calculations for single-crystalline polymers[2].

We have shown that to quantitatively describe the strain as a function of electric field, the additional term $d_{\text{coupling}}E\acute{p}$ has to be included. This term can be due to any process that yields a strain that depends linearly on electric field and changes direction at the coercive field. The mechanism could be, for instance, internal Maxwell stress, interface polarization[22], dielectric and/or piezoelectric Maxwell–Wagner relaxations[23,24] and piezoelectrically induced mechanical interactions[14]. We tentatively propose that this additional contribution originates from the composite structure of the polymer—that is, the coexistence of the crystalline and amorphous phase. As shown in Supplementary Section 5 the microstructure of PVDF films consists of huge lamellae, sheets of crystals that grow outwards starting from a central nucleation site. In between the lamellae is the amorphous phase. The copolymer P(VDF-TrFE) crystallizes in needle-like domains. Details of the packing and folding of the polymer chains are not completely known, but as in PVDF the amorphous and crystalline phases seem to be intermixed.

In a simplified microscopic representation, we consider the film as consisting of alternating crystalline and amorphous slabs. The polarization is due to the dipoles of the crystalline lamellae. The amorphous slab is a linear dielectric. We consider a comprising capacitor. The electric field of the polar lamellae induces a surface

charge $\pm Q$ at the top and bottom electrodes. For the sake of explanation, we consider the thermodynamically equivalent direct piezoelectric effect. Assume a compressive stress is applied that decreases the thickness. Part of the deformation is accommodated by contraction of the amorphous matrix. The concomitant increase of the capacitance dictates that the charges on the electrodes are adjusted by $\pm\Delta Q$. Temporarily there is current flowing through the circuit. The additional charge corresponds to an electric field in the direction of the polarization. The contraction in tandem with the relative orientation of the polarization and the electric field correspond to a negative piezoelectric coefficient, reflected in the additional d_{coupling} term. Because the amorphous parts and the lamellae are not independent but strongly intertwined, this contraction can be regarded as an internal compressive stress to the lamellae, leading to a further reduction of the lattice constant.

Hence, in summary, when an electric field is applied over PVDF or its copolymers, the crystalline lamellae contract as a result of electrostriction, the dipole-induced piezoelectricity. The lattice constant decreases. However, in addition, the amorphous parts in between the polar lamellae contract. This contraction can be regarded as an additional, internal compressive stress to the lamellae, leading to a further reduction of the lattice constant. In the first-order approximation this additional strain will increase with electric field and therefore can be described by an additional term, $d_{\text{coupling}}E\acute{p}$, where the proportionality constant is negative. The piezoelectric coefficient, d_{33}, is negative, as both comprising coefficients, d_{coupling} and Q_{33}, are negative.

To support the analysis, we show that the effect depends on the microstructure of the polymer. For this purpose we fabricated capacitors of thick P(VDF-TrFE) films and varied the annealing temperature to control the crystallinity. The microstructure was investigated with DSC and XRD measurements. We measured the strain simultaneously with the displacement as a function of electric field and we modelled the strain according to equation (2). All measurements could be quantitatively interpreted. The data are presented in Supplementary Section 12. The extracted electrostrictive coefficient, Q_{33}, can be linked to the Young's modulus, and the piezoelectric coefficients, d_{coupling} and d_{33}, vary with the remanent polarization.

In summary, we have performed *in situ* dynamic X-ray diffraction measurements on P(VDF-TrFE) capacitors. The strain, as derived from the change in lattice constant with electric field, is comparable to reported strain measured interferometrically on bulk samples. Hence, the piezoelectric effect is dominated by the change in lattice constant but, surprisingly, it cannot be accounted for by the electrostrictive response of the crystalline part alone. An additional contribution, $d_{\text{coupling}}E\acute{p}$, has to be included to quantitatively describe the strain for all values of the electric field. We argue that its origin is the electromechanical coupling between the intermixed crystalline lamellae and amorphous regions of the semicrystalline polymers. The piezoelectric coefficient, d_{33}, is negative, as both comprising coefficients, the electrostrictive, Q_{33}, as well as the additional, d_{coupling}, are negative. Our findings tie the negative piezoelectric response of PVDF and its copolymers to the dynamics of their composite microstructure.

Methods

Methods and any associated references are available in the online version of the paper.

Received 17 December 2014; accepted 14 August 2015; published online 5 October 2015

References

1. Furukawa, T. & Seo, N. Electrostriction as the origin of piezoelectricity in ferroelectric polymers. *Jpn. J. Appl. Phys.* **29,** 675–680 (1990).
2. Bystrov, V. S. *et al.* Molecular modeling of the piezoelectric effect in the ferroelectric polymer poly(vinylidene fluoride) (PVDF). *J. Mol. Model.* **19,** 3591–3602 (2013).
3. Wada, Y. & Hayakawa, R. A model theory of piezo- and pyroelectricity of poly(vinylidene fluoride) electret. *Ferroelectrics* **32,** 115–118 (1981).
4. Furukawa, T., When, J. X., Suzuki, K., Takashina, Y. & Date, M. Piezoelectricity and pyroelectricity in vinylidene fluoride/trifluoroehtylene copolymers. *J. Appl. Phys.* **56,** 829–834 (1984).
5. Broadhurst, M. G. & Davis, G. T. Physical basis for piezoelectricity in PVDF. *Ferroelectrics* **60,** 3–13 (1984).
6. Ejdrup, T. *et al.* Picosecond time-resolved laser pump/X-ray probe experiments using a gated single-photon-counting area detector. *J. Synchrotron Radiat.* **16,** 387–390 (2009).
7. Haldrup, K. *et al.* Guest–host interactions investigated by time-resolved X-ray spectroscopies and scattering at MHz rates: Solvation dynamics and photoinduced spin transition in aqueous $Fe(bipy)_3^{2+}$. *J. Phys. Chem. A* **116,** 9878–9887 (2012).
8. Wurfel, P. & Batra, I. P. Depolarization-field-induced instability in thin ferroelectric films—experiment and theory. *Phys. Rev. B* **8,** 5126–5133 (1973).
9. Lines, M. E. & Glass, A. M. *Principles and Applications of Ferroelectrics and Related Materials* (Oxford Univ. Press, 1977).
10. Stengel, M., Spaldin, N. A. & Vanderbilt, D. Electric displacement as the fundamental variable in electronic-structure calculations. *Nature Phys.* **5,** 304–308 (2009).
11. Devonshire, A. F. Theory of barium titanate—Part II. *Philos. Mag.* **42,** 1065–1079 (1951).
12. Newnham, R. E., Sundar, V., Yimnirun, R., Su, J. & Zhang, Q. M. Electrostriction: Nonlinear electromechanical coupling in solid dielectrics. *J. Phys. Chem. B* **101,** 10141–10150 (1997).
13. Li, F., Jin, L., Xu, Z. & Zhang, S. Electrostrictive effect in ferroelectrics: An alternative approach to improve piezoelectricity. *Appl. Phys. Rev.* **1,** 11103–11121 (2014).
14. Pramanick, A., Damjanovic, D., Daniels, J. E., Nino, J. C. & Jones, J. L. Origins of electro-mechanical coupling in polycrystalline ferroelectrics during subcoercive electrical loading. *J. Am. Ceram. Soc.* **94,** 293–309 (2011).
15. Miller, S. L. & McWhorter, P. J. Physics of the ferroelectric nonvolatile memory field effect transistor. *J. Appl. Phys.* **72,** 5999–6010 (1992).
16. Lue, H.-T., Wu, C.-J. & Tseng, T.-Y. Device modeling of ferroelectric memory field-effect transistor (FeMFET). *IEEE Trans. Electron Dev.* **49,** 1790–1798 (2002).
17. Brondijk, J. J., Asadi, K., Blom, P. W. M. & de Leeuw, D. M. Physics of organic ferroelectric field-effect transistors. *J. Polym. Sci. B* **50,** 47–54 (2012).
18. Kepler, R. G. *Ferroelectric Polymers*, Ch. 3 (Marcel Dekker, 1995).
19. Tagantsev, A. K., Cross, L. E. & Fousek, J. *Domains in Ferroic Crystals and Thin Films* (Springer, 2010).
20. Cross, L. E. *Ferroelectric Ceramics: Tailoring Properties for Specific Applications* (Birkhäuser, 1993).
21. Lindner, M. *et al.* Charged cellular polymers with ferroelectric behaviour. *IEEE Trans. Dielectr. Electr. Insul.* **11,** 255–263 (2004).
22. Rollik, D., Bauer, S. & Gerhard-Multhaupt, R. Separate contributions to the pyroelectricity in polyvinylidene fluoride from the amorphous and crystalline phases, as well as from their interface. *J. Appl. Phys.* **85,** 3282–3288 (1999).
23. Ueda, H., Fukada, E. & Karasz, F. E. Piezoelectricity in three-phase systems: Effect of the boundary phase. *J. Appl. Phys.* **60,** 2672–2677 (1986).
24. Turik, A. V. & Radchenko, G. S. Maxwell–Wagner relaxation in piezoactive media. *J. Phys. D: Appl. Phys.* **35,** 1188–1192 (2002).

Acknowledgements

We gratefully acknowledge P. Groen from the Holst Centre, TNO, The Netherlands, for stimulating discussions on inorganic piezoelectrics and ferroelectrics. We are indebted to H. Wondergem, Philips Research, Eindhoven, The Netherlands for X-ray analysis of P(VDF-TrFE) films and to G. Glasser from the Max Plank Institute for Polymer Research, Mainz, Germany, for the SEM micrographs. We acknowledge H. Lemke, currently at the SLAC National Accelerator Laboratory, for his contributions, the beamline scientists A. Beerlink and O. Seeck, as well as the excellent technical support received at P08 at PETRA III, Hamburg. We acknowledge financial support from the Zernike Institute for Advanced Materials, by KAU from project 71-100-35-HiCi, by the EC under FP7 contract no. 212311, ONE-P and by the Max Planck Institute for Polymer Research. K.S.K., T.B.v.D., Y.G. and M.M.N. acknowledge support from DANSCATT. T.B.v.D. and M.M.N. acknowledge support from the ReLiable project (Project No. 11-116792) funded by the Danish Council for Strategic Research Programme Commission on Sustainable Energy and Environment. K.A. acknowledges the Alexander von Humboldt Foundation for the funding provided in the framework of the Sofja Kovalevskaja Award endowed by the Federal Ministry of Education and Research, Germany. D.D. acknowledges support from the Swiss National Science Foundation (No. 200021-159603).

Author contributions

D.M.d.L. and M.M.N. conceived the idea and designed the experiments. M.L., K.A., D.Z., T.L. and I.K. fabricated and characterized the ferroelectric capacitors. T.B.v.D., K.S.K. and Y.G. performed the synchrotron measurements. I.K. modelled the data. D.D. supervised the theoretical analysis. I.K., K.A., M.L., T.B.v.D., K.S.K., Y.G., P.W.M.B., D.D., M.M.N. and D.M.d.L. co-wrote and commented on the manuscript. I.K. and D.M.d.L. supervised the project.

Additional information

Supplementary information is available in the online version of the paper. Reprints and permissions information is available online at www.nature.com/reprints. Correspondence and requests for materials should be addressed to D.M.d.L.

Competing financial interests

The authors declare no competing financial interests.

Methods

Dynamic *in situ* grazing incidence X-ray diffraction measurements (GI-XRD) were performed on P(VDF-TrFE) (65–35%) capacitors as schematically depicted in Fig. 2. Details of the fabrication are presented in Supplementary Section 3. To prevent parasitic diffraction patterns we used single-crystalline quartz as a substrate, Pd as a bottom electrode and PEDOT:PSS, a water-based suspension of poly(3,4-ethylenedioxythiophene) stabilized with poly(4-styrenesulphonic acid), as a non-diffracting top electrode.

In situ grazing incidence X-ray diffraction measurements (GI-XRD) were conducted at the High Resolution Diffraction Beamline P08 at PETRAIII, Deutsches Elektron Synchrotron (DESY), Hamburg. A section near the specular plane of the out-of-plane scattering, from the coinciding (200) and (110) Bragg peaks of the aligned sample, was recorded on a time-gated Pilatus 100K pixel detector, read out at ~100 Hz. We have previously used similar gating techniques to obtain time resolutions below ~100 ps (refs 6,7). The scattering vector was measured while displacement loops versus electric field of the samples were recorded using a Sawyer–Tower circuit. For each measurement, 10,000 scattering images were recorded, with an integration time of a few milliseconds per image. Details of the dynamic *in situ* X-ray measurements and the data acquisition procedure are presented in Supplementary Section 6. By synchronizing the recording of the X-ray images to the driving electric field, the scattering could be measured as a function of the instantaneously applied bias.

A triangular waveform was used to drive the ferroelectric capacitors. The applied a.c. voltage and the capacitor response were recorded as a function of time using the oscilloscope of the Sawyer–Tower system. The X-ray detector started recording after a trigger signal at the zero-crossing (rising edge) of the applied bias. The trigger pulse, as well as a TTL signal mirroring the Pilatus exposures, was also recorded by the oscilloscope of the Sawyer–Tower set-up. The Bragg peak position was extracted from the X-ray data and synchronized with the electrical data using the oscilloscope traces. Subsequently, the capacitor response (displacement current), the driving signal (applied electric field) and the Bragg peak position (strain) were interpolated and averaged according to a single cycle of the driving signal. Details of the data synchronization procedure are presented in Supplementary Section 7.